Journal of Materials Chemistry A

Dynamic Article Links ►

Cite this: DOI: 10.1039/c0xx00000x

ARTICLE TYPE

www.rsc.org/xxxxxx

Synthesis of carbon nanotubes by microwave heating 4[†‡]: Influence of diameter of catalytic Ni nanoparticles on diameter of CNTs

Kazuchika Ohta,*[a] Toshiki Nishizawa,[a] Takahiro Nishiguchi,[a] Ryo Shimizu,[b] Yoshiyuki Hattori,[b] Shuji Inoue,[c] Masakazu Katayama,[c] Kazuhiko Mizu-uchi[c] and Takumi Kono[c]

Received (in XXX, XXX) Xth XXXXXXXXX 20XX, Accepted Xth XXXXXXXXX 20XX
DOI: 10.1039/b000000x

We have rapidly synthesized multi wall carbon nanotubes (MWCNTs) by calcination of granulated polystyrene with nickel nanoparticles having different average diameter ($\mathbf{D_{Ni}}$ = 10, 20, 50 or 90 nm) under nitrogen gas at a certain temperature and time, (700°C, 15 min) or (800°C, 10 min), using a domestic microwave oven in order to systematically investigate influence of the diameter of nickel nanoparticles on the diameter of MWCNTs. The MWCNTs synthesized here were characterized by a transmission electron microscope, a Raman spectrophotometer and a wide angle X-ray diffractometer. We found that for the calcination condition of (800°C, 10 min), a relationship between the outer diameter of the resulted carbon nanotubes ($\mathbf{D_{CNT}}$) and the diameter of catalytic nickel nanoparticles ($\mathbf{D_{Ni}}$) can be described as a linear function, $D_{CNT} = 1.01D_{Ni}+14.79$ nm with the correlation coefficient R = 0.99, and that for the calcination condition of (700°C, 15 min), $D_{CNT} = 1.12D_{Ni}+7.80$ nm with R = 0.95. Thus, we revealed that when diameter of the catalytic nickel nanoparticles ($\mathbf{D_{Ni}}$) increases by 1 nm, the outer diameter of the obtained MWCNTs ($\mathbf{D_{CNT}}$) increases by about 1 nm.

1. INTRODUCTION

In recent years, carbon nanotubes (CNTs) have been very much paid attention as new carbon materials because they have various excellent properties in electroconductivity, thermal conductivity, chemical stability, etc.[1, 2] The names of CNTs change by the number of walls like as single wall carbon nanotube (SWCNT), double wall carbon nanotube (DWCNT), and multi wall carbon nanotube (MWCNT). The properties change by the number of walls and symmetry of the layer.[1, 2] As the synthetic methods of CNTs, arc discharge method,[3-6] layer ablation method,[7] and chemical vapour deposition(CVD) method[8, 9] have been world-widely developed up to date. However, each method needs high energy and expensive apparatuses.[1-9] On the other hand, we have developed four convenient rapid synthetic methods, "metal complex method",[10] "mixture method",[10] "nano fiber method",[11] and "nickel nanoparticle method",[12] by microwave heating using a cheap domestic microwave oven. When these methods were employed, MWCNTs could be synthesized in much lower cost with saving energy within extremely short time. The nickel nanoparticle method was the most rapid and energy-saving one among these four methods. We could readily synthesize MWCNTs from commercially available granulated polystyrene (PS) and nickel nanoparticles in a very short time by using a domestic microwave oven remodeled to control the temperature. Therefore, we have pursued the best condition to synthesize MWCNTs by using this nickel nanoparticle method.[12] In order to establish the best conditions for the synthesis of MWCNTs, we carried out the syntheses with changing temperature from 600 to 900°C and/or time from 5 to 20 min of microwave heating, and then the qualities of the resulting MWCNTs were checked by TEM, Raman spectroscopy and X-ray diffraction. As a result, it was clarified that the best condition was at 800°C for 10 min, and that the second best one was at 700°C for 15 min. Under the best condition, we could easily synthesize MWCNTs in gram scale at a time, when the total amount of the mixture of PS and nickel nanoperticles increased to several grams with keeping the nickel weight ratio at 0.30. This may lead us to a bright prospect of rapid synthesis of large amounts of CNTs in kilogram scale by using a large-scale reactor in a factory. However, the diameters of the obtained MWCNTs were about 25~100 nm. Thus, we could not control the diameters of the MWCNTs synthesized by using this method in our previous work.[12] We thought that it might be attributed to the largely distributed diameters (average = 100 nm) of the catalytic nickel nanoparticles used in our previous work.

As known well, in order to synthesize CNTs all the methods need metal catalyst like as Fe, Co, Ni, etc. It has been reported that the diameter of CNTs depends on the diameter of the catalytic metal nanoparticles, but there have been very few systematic studies of this effect.[13-15] It may be attributed to difficulty of preparation of the catalytic metal nanoparticles having desired diameter. Recently, a joint research group of Osaka University and Nippon Steel & Sumikin Chemical Co. Ltd. has successfully prepared the nickel nanoparticles having desired

diameter in a very narrow distribution by microwave heating of octanol solution of the Ni[(dialkylamino)(diformato)] ($Ni[(RNH_2)_2(HCOO)_2]$) complexes having different alkyl chain length.[16] We have obtained the nickel nanoparticles having four different diameters (10, 20, 50 and 90 nm) from this group, and systematically investigated effect of the diameter ($\mathbf{D_{Ni}}$) of catalytic nickel nanoparticles on the diameter ($\mathbf{D_{CNT}}$) of MWCNTs in this work.

2. EXPERIMENTAL

2-1. Apparatuses

The microwave heating apparatus used in this work is illustrated in Fig.1. As shown in this figure, a commercially available domestic microwave oven (Sharp RE-T1(700W)) was remodeled in order to control the temperature, by using a thermocouple and a temperature controller.[10] In this microwave oven was placed a furnace of Art Box™ which can be heated by microwave irradiation.[17] A quartz test tube (diameter = 15 nm, length = 180

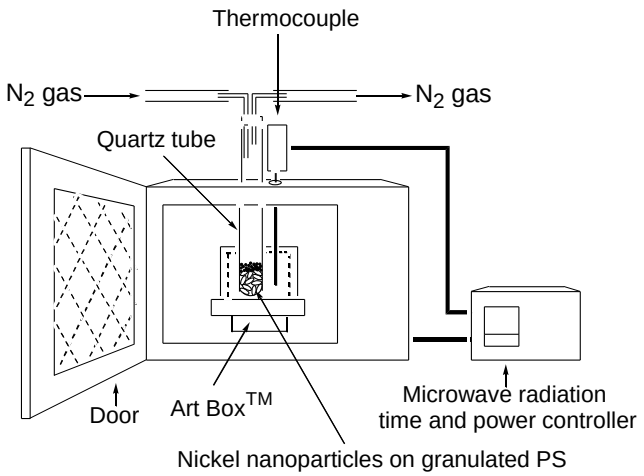

Fig. 1. Setup for synthesis of carbon nanotubes by using a remodeled domestic microwave oven and an Art Box™.

nm) was inserted into this box, and nitrogen gas was pumped through this test tube as a reactor vessel.

2-2. Synthesis

Into a quartz test tube, 0.70 g of granulated polystyrene (PS: Wako Chemicals, polymerization degree = *ca*.2000) and 0.30 g of nickel nanoparticles (Nippon Steel & Sumikin Chemical, NSCC-10(average diameter = 10nm), NSCC-20(20nm), NSCC-50(50nm) or NSCC-90(90nm)) were sequentially put. Nitrogen gas was pumped through the air. When an Art Box set in the domestic oven, it was irradiated by microwave so the temperature inside the box reached the desired temperature (700 or 800°C), this test tube was inserted into the Art Box. PS was calcinated for a certain period (10 or 15 minutes) under nitrogen gas. After spontaneously cooling to r.t., 10 ml of conc. hydrochloric acid (36% aq. sol.) was poured into this test tube and immersed in an ultrasonic washing machine (Sharp: UT-105S) for one hour to resolve the remaining bare nickel nanoparticles. The contents were moved into an Erlenmeyer flask and left overnight. Into this flask, 50 ml of water was poured and the resulted suspension was divided into several centrifuge tubes. After separation of the suspension into the black participates and the acidic water by using a centrifugal separator (Shimadzu: CPN-005), the acidic water layer was decanted and flesh water was added. This manipulation was repeated until the aqueous layer became neutral. The collected black residue was dried in a dryer (Fine: FO-60W) at 140°C for overnight, and then further dried under vacuum at r.t. for 2 more hours to afford black carbon products. Table 1 lists the average yields (mg) of carbon products. For each of the conditions (nickel nanoparticles size, temperature and time), it was carried out five times. Each of the average values was calculated from three mean values excluding the maximum and minimum values.

Table 1 Yields of carbon products depending on diameter of nickel nanoparticle ($\mathbf{D_{Ni}}$), calcination temperature and heating time.

Temp. (°C)	Heating time (min)	D_{Ni} (nm)			
		10	20	50	90
		Yield (mg)			
800	10	63.9	66.3	83.2	87.5
700	15	64.7	64.9	81.0	82.2

[a] Each of the yields was the average of three mean values excluding the biggest and smallest values, among five measured values.

2-3. Characterization

The black carbon products prepared here were characterized by a transmission electron microscope (JEOL, 2010 Fas TEM microscope), a Raman spectrophotometer (Holo Lab 5000) and a wide angle X-ray diffractometer (Rigaku, Rad).

3. RESULTS AND DISCUSSION

3-1. Yields

As can be seen from Table.1, both of the conditions of (800°C, 10 min) and (700°C, 15 min) gave higher yield (mg) of the carbon products with increasing the nickel nanoparticle diameter ($\mathbf{D_{Ni}}$). The bigger the nickel nanoparticle diameter becomes, the more the carbon atoms resolve in the nickel nanoparticle, because the volume of nickel nanoparticle rapidly increases in proportion to the third power of the diameter. Therefore, the more carbon products can be formed from the bigger nickel nanoparticles. This will be discussed in details in Section 3-5.

3-2. TEM observation

3-2-1 TEM images

Figs.2 and 3 show the representative TEM images of MWCNTs synthesized for the conditions of (700°C, 15 min) and (800°C, 10 min), respectively. As can be seen from these TEM images, the bigger the nickel nanoparticle diameter ($\mathbf{D_{Ni}}$) becomes, the bigger the outer diameter of the synthesized MWCNTs ($\mathbf{D_{CNT}}$) becomes. Fig.4 shows nomenclature of the distances in MWCNT. Fig.4[A] schematically illustrates the distances: $\mathbf{D_{CNT}}$ = outer diameter of MWCNT, **r** = inner diameter of MWCNT, **L** = wall thickness, **n** = the number of graphene layers, and **l** = graphene thickness. Fig.4[B] shows an example of the MWCNT in Sample No. 26 listed in Table S1. It could be estimated from this image that $\mathbf{D_{CNT}}$, **r**, **L**, **n** and **l** are 32.8, 12.1, 10.0, 28 and 0.357 nm, respectively. In Table S1 are listed 64 sets of the measured values

This journal is © The Royal Society of Chemistry [year]

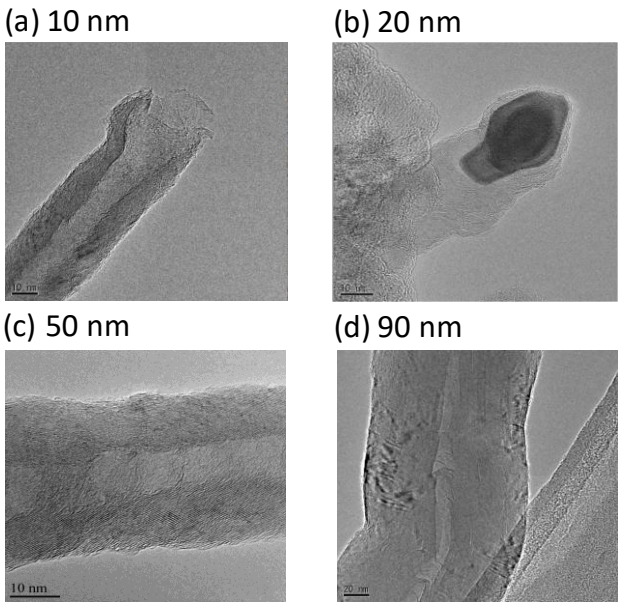

Fig. 2 TEM images of CNT obtained for calcination at 700°C for 15min by using different nano Ni diameters ($\mathbf{D_{Ni}}$), 10, 20, 50, and 90 nm.

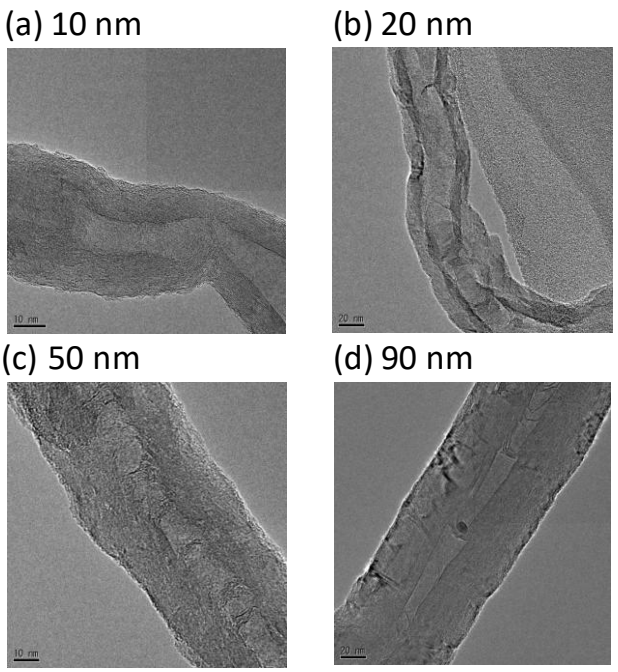

Fig. 3 TEM images of CNT obtained for calcination at 800oC for 10min by using different nano Ni diameters ($\mathbf{D_{Ni}}$), 10, 20, 50 and 90 nm.

of $\mathbf{D_{CNT}}$, **r**, **L** and **n**, and the calculated values of **l** of the MWCNTs synthesized with changing the diameter of nickel nanoparticle like 90→50→20→10 nm at a certain calcinations condition, (700°C, 15 min) or (800°C, 10 min). These values were obtained from the TEM images.

3.2.2. Outer diameter of MWCNT ($\mathbf{D_{CNT}}$)

In Fig.5, the outer diameters ($\mathbf{D_{CNT}}$) are plotted against the nickel nanoparticle diameters ($\mathbf{D_{Ni}}$). Fig.5[A] and [B] show the relationship between $\mathbf{D_{CNT}}$ and $\mathbf{D_{Ni}}$, for the calcinations conditions of (800°C, 10 min) and (700°C, 15 min), respectively. In the figure, the values denoted as cross (x) mark and filed circle

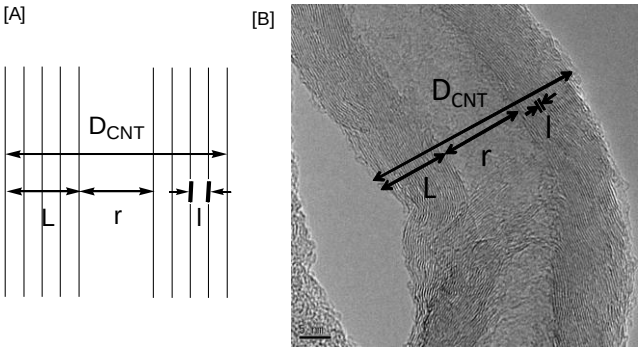

Fig. 4 [A] Nomenclature of the distances in MWCNT: $\mathbf{D_{CNT}}$ = outer diameter of MWCNT, **r** = inner diameter of MWCNT, **l** = thickness of a graphene, and **L** = wall thickness. **L** = n**l** (n = number of graphene layers); [B] Example of the MWCNT in Sample No. 26 listed in Table S1: $\mathbf{D_{CNT}}$ = 32.8, **r** = 12.1, **L** = 10.0 nm, n = 28 and **l** = 0.357 nm.

(●) are the observed and average values, respectively. As can be seen from this figure, the outer diameter of MWCNTs ($\mathbf{D_{CNT}}$) linearly increases with increasing the diameter of nickel nanoparticles ($\mathbf{D_{Ni}}$) for both the calcination conditions.

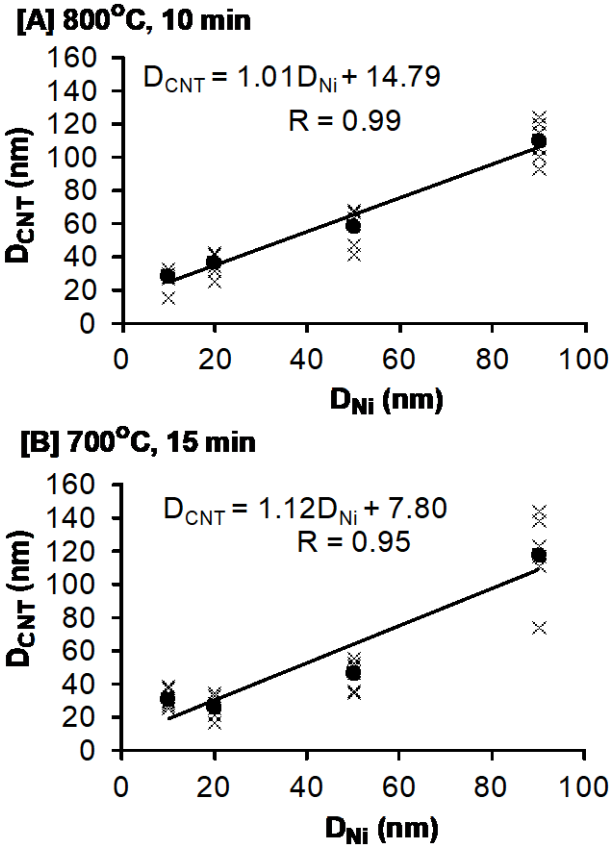

Fig. 5 Outer diameter of the obtained CNTs ($\mathbf{D_{CNT}}$) versus diameter the Ni nanoparticle ($\mathbf{D_{Ni}}$): [A] 800°C, 10 min, [B] 700°C, 15 min. x = measured value and ● = the average value.

As can be seen from Fig.5[A], a relationship between the average values of $\mathbf{D_{CNT}}$ for (800°C, 10 min) and the $\mathbf{D_{Ni}}$ values could be obtained as a linear function, D_{CNT} = 1.01D_{Ni}+14.79, and the correlation coefficient R is 0.99, which means that $\mathbf{D_{CNT}}$ and $\mathbf{D_{Ni}}$ show an excellent correlation. Since the slope is 1.01, the outer diameter of the resulted MWCNTs for (800°C, 10 min)

increases by 1.01 nm when the diameter of nickel nanoparticles increases by 1.00 nm. As can be seen from Fig.5[B], a relationship between the average values of $\mathbf{D_{CNT}}$ for (700°C, 15 min) and the $\mathbf{D_{Ni}}$ values can be similarly obtained as a linear function, $D_{CNT} = 1.12D_{Ni}+7.80$, R = 0.95, which means that $\mathbf{D_{CNT}}$ and $\mathbf{D_{Ni}}$ also show a satisfactory correlation. Since the slope is 1.12, the outer diameter of the resulted MWCNTs for (700°C, 15 min) increases by 1.12 nm when the diameter of nickel nanoparticles increases by 1.00 nm. It has been reported in Figure 24 and Table 4 of the review paper[14] that the outer diameter of the CNTs ($\mathbf{D_{CNT}}$ = 1.0~11.7 nm) appeared in several papers also gave linearity with the diameter of the catalytic metal nanoparticles ($\mathbf{D_M}$ = 1.0~12.6 nm). By using the values reported in Table 4 in this review, a liner function, $D_{CNT} = 0.92D_M-0.50$; R=1.00, could be obtained. The correlation coefficient R=1.00 means extremely excellent correlation between $\mathbf{D_{CNT}}$ and $\mathbf{D_M}$. When the diameter of catalytic metal nanoparticles ($\mathbf{D_M}$) increases by 1.0 nm, the outer diameter of the resulted CNTs ($\mathbf{D_{CNT}}$) increases by 0.92 nm. Therefore, it became apparent from these linear functions in both the previous works and our present work that when diameter of

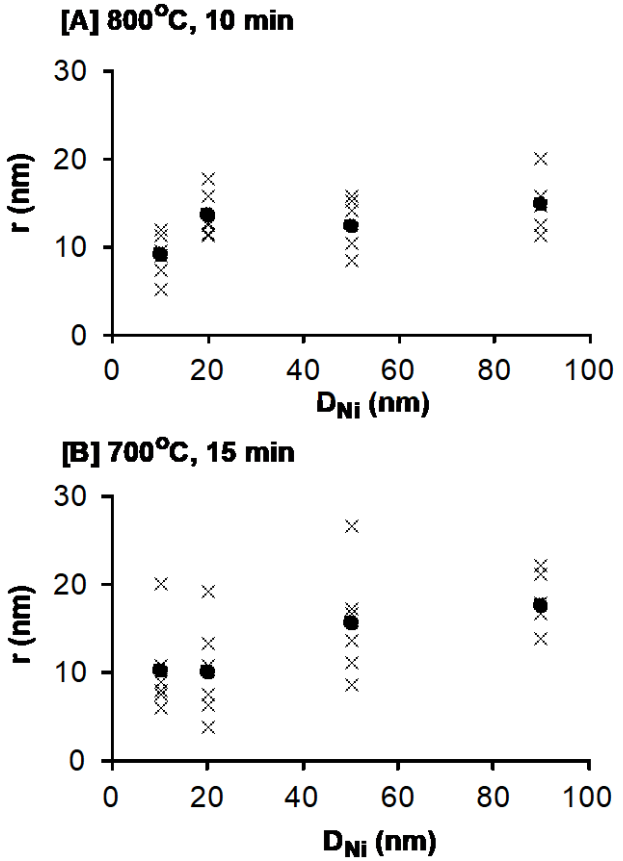

Fig. 6 Inner diameter (**r**) of the obtained CNTs versus diameter of the Ni nanoparticle ($\mathbf{D_{Ni}}$): [A] 800°C, 10 min, [B] 700°C, 15 min. x = measured value and ● = the average value.

the catalytic metal nanoparticles ($\mathbf{D_M}$) increases by 1 nm in the wide range from 1nm to 90nm, outer diameter of the resulted CNTs ($\mathbf{D_{CNT}}$) increases by about 1 nm. To our best knowledge, such a good linearity between $\mathbf{D_M}$ and $\mathbf{D_{CNT}}$ has been established at the first time in such a very wide range of diameter of catalytic metal nanoparticles.

3-2-3. Inner diameter of MW CNT (r)

In Fig.6, the inner diameters (**r**) of the resulted MWCNTs are plotted against the nickel nanoparticle diameters ($\mathbf{D_{Ni}}$). Fig.6[A] and [B] show relationship of (800°C, 10 min) and (700°C, 15 min), respectively. As can be seen from this figure, each of them shows a big scatter. However, the dispersion of the **r** values for (800°C, 10 min) is smaller than that for (700°C, 15 min). Hence, the calcination condition of (800°C, 10 min) may be more suitable than that of (700°C, 15 min).

3-2-4. Wall thickness (L)

In Fig.7, the observed values of wall thickness (**L**) are plotted against the nickel nanoparticle diameters ($\mathbf{D_{Ni}}$). Fig.7[A] and [B] show the graphs for the calcinations conditions of (800°C, 10 min) and (700°C, 15 min), respectively. As can be seen from these graphs, the wall thickness (**L**) increases with increasing the nickel nanoparticle diameter ($\mathbf{D_{Ni}}$), similarly to the outer diameter of MWCNT ($\mathbf{D_{CNT}}$).

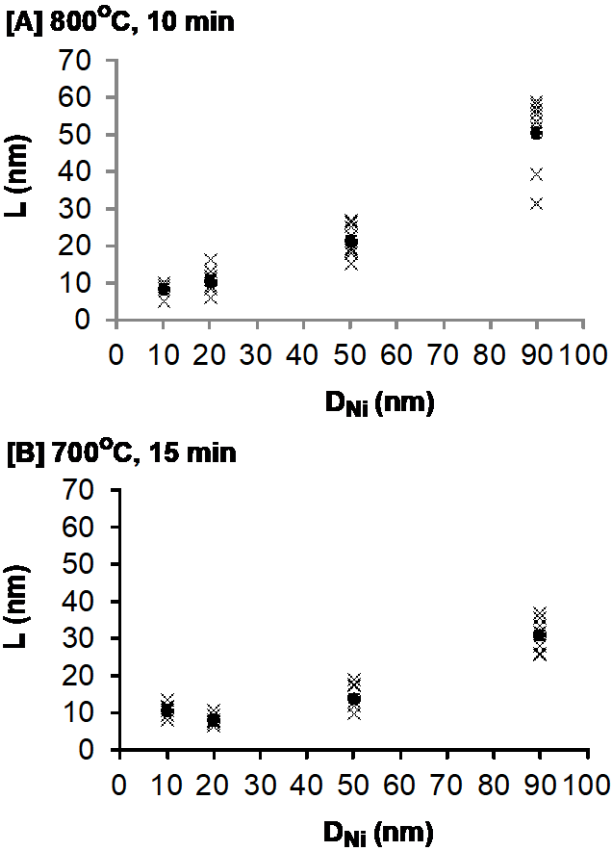

Fig.7 Wall thickness (**L**) of the obtained CNTs versus diameter of Ni nanoparticles: ($\mathbf{D_{Ni}}$): [A] 800°C, 10 min; [B] 700°C,15 min. x = measured value and ● = the average value.

3-2-5. Number of graphene layers (n)

The number of graphene layers (**n**) was counted from each of the TEM images. The observed numbers (**n**) are plotted against the nickel nanoparticle diameters ($\mathbf{D_{Ni}}$) in Fig.8. As can be seen from this figure, the number (**n**) increases with increasing the $\mathbf{D_{Ni}}$ value, similarly to the $\mathbf{D_{CNT}}$ value.

3-2-6. Graphene thickness (l)

The graphene thickness (**l**) could be calculated from an equation of **l** = **L**/**n**. The calculated **l** values are also listed in Table S1, and plotted against the $\mathbf{D_{Ni}}$ values in Fig.9. As can be seen from these table and figure, the **l** values of graphene thickness are almost

This journal is © The Royal Society of Chemistry [year]

constant at about 0.35 nm as the same as the generally observed values.

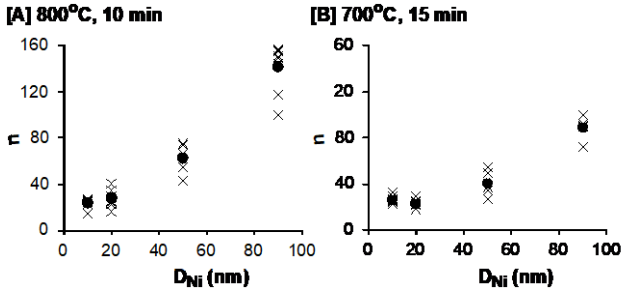

Fig.8 The number of grapheme layers (**n**) of the obtained CNTs versus diameter of Ni nanoparticles ($\mathbf{D_{Ni}}$): [A] 800°C, 10 min; [B] 700°C, 15 min. x = measured value and ● = the average value.

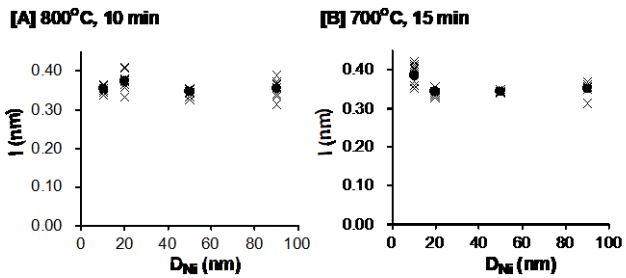

Fig.9 The calculated values of graphene thickness (**l** = **L**/**n**) of the obtained CNTs versus diameter of Ni nanoparticles ($\mathbf{D_{Ni}}$): [A] 800°C, 10 min; [B] 700°C, 15 min. x = measured value and ● = the average value.

3-3. X-ray diffraction studies

Fig.10 shows the X-ray diffraction patterns of the carbon products obtained by calcinations in the conditions of (700°C, 15 min) and (800°C, 10 min) with changing the diameter of catalytic nickel nanoparticles ($\mathbf{D_{Ni}}$). We focused on two reflection peaks of Ni(111) and graphite(002). The Ni(111) reflection can be attributed to nickel metal encapsulated in the carbon products, because the bare nickel metal was completely removed from the product when it had been treated by conc. hydrochloric acid aq. solution during the purification. As can be seen from this figure, the intensity of the graphite(002) reflection increases with increasing the diameter of nickel nanoparticles ($\mathbf{D_{Ni}}$) for both of the calcinations conditions. To further clarify this tendency, intensity ratios of Gr(002)/Ni(111) [12] are plotted against the diameter of nickel nanoparticles ($\mathbf{D_{Ni}}$) in Fig.S1. As can be seen from this figure, the Gr(002)/Ni(111) ratios obviously increase with increasing the diameter $\mathbf{D_{Ni}}$. This means that the graphene structure develops with increasing the diameter of the nickel nanoparticles. It may be attributed to the volume of nickel nanoparticles, as already pointed out also in Section 3.1. Since the volume of nickel nanoparticles rapidly increases in proportion to the third power of the diameter of $\mathbf{D_{Ni}}$, the more the carbon atoms resolve in the nickel nanoparticles and the more carbon products may be originated. This will be discussed in details in Section 3-5.

3-4. Raman spectra

Fig.11 shows Raman spectra of the carbon products obtained by calcination in the conditions of (800°C, 10 min) and (700°C, 15 min) with changing the $\mathbf{D_{Ni}}$ diameter. Each of the spectra gave a G band due to graphene and a D band due to defect of the

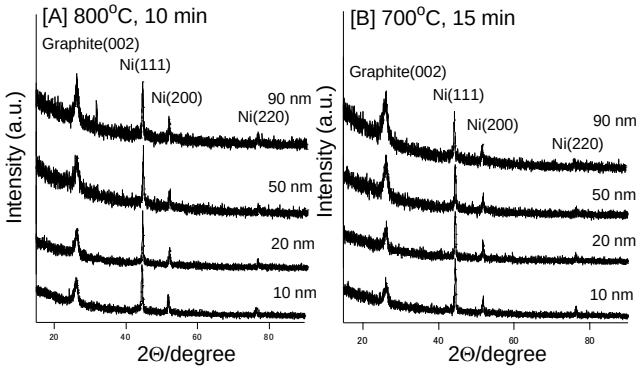

Fig.10 X-ray diffraction patterns of the carbon products obtained by using different diameter of catalytic Ni nanoparticle: [A] 800°C, 10 min, [B] 700°C, 15 min. The intensities of Ni(111) are normalized in these graphs.

graphene. Compared to the intensity of G band, the intensity of D band relatively increases with increasing the $\mathbf{D_{Ni}}$ diameter for both of the calcination conditions. To further clarify this tendency, the peak intensity ratios of D/G are plotted against the $\mathbf{D_{Ni}}$ diameters in Fig.S2. As can be seen from this figure, the D/G intensity ratio obviously increases with increasing the diameter of nickel nanoparticle ($\mathbf{D_{Ni}}$), in a sequence of 20→50→90 nm for both of the calcination conditions. Thus, the more defective MWCNTs were produced with increasing the D_{Ni} diameter. For 10→20 nm, the D/G intensity ratios slightly decrease for both of the conditions. The reason is not clear at the present time. Further studies are necessary.

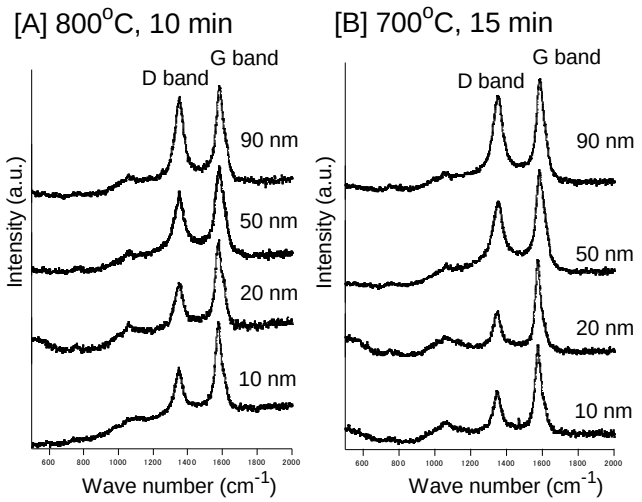

Fig.11 Raman spectra of the carbon products obtained by using different diameter of Ni nanoparticles ($\mathbf{D_{Ni}}$): [A] 800°C, 10 min, [B] 700°C, 15 min.

3-5. Possible production mechanism of CNTs

As illustrated in Fig. 12, when granulated polystyrene is heated at 700°C or 800°C, it decomposes to atomic carbons, which resolve into nickel nanoparticles to form a **solid solution** between nickel and carbon. On cooling, the supersaturated carbon recrystallizes from the **solid solution** of nanoparticles to form carbon nanocapsules and/or carbon nanotubes on the surface of nickel nanoparticles. On further cooling, carbon nanotubes continue to grow by separating saturated carbon from the **solid solution**. Therefore, solubility of carbon in metal may be crucial point for carbon nanotube production.

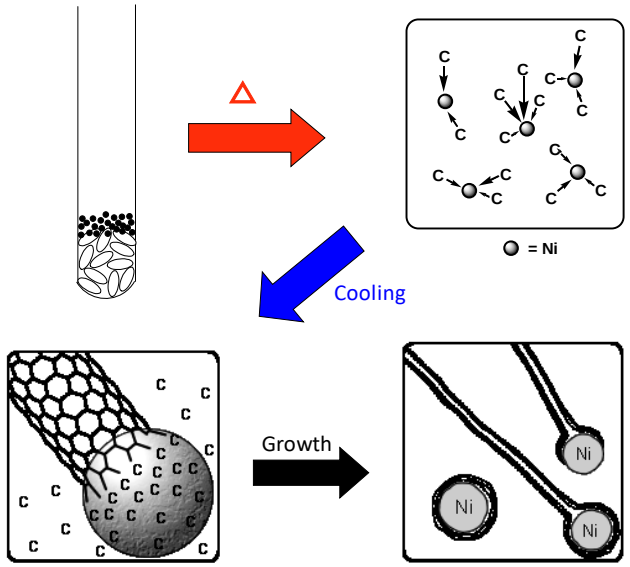

Fig.12 Schematic illustration of the production mechanism of CNTs by calcination of polystyrene with nickel nanoparticles.

Fig. 13 shows metal-carbon phase diagrams for Fe, Co,Ni and Cu.[18] Coloured area represents **solid solution**. As can be seen from these diagrams, each of the metals, Fe, Co and Ni, can form **solid solution**, whereas Cu does not form the **solid solution**. It is consistent with the fact that Fe, Co and Ni are catalysts for carbon nanotube synthesis but Cu is not. Hence, it is apparent that catalytic ability for carbon nanotube synthesis may be originated from ability of formation of **solid solution** between metal and carbon.

Hereupon, we consider physical meaning of recrystallization and phase separation from thermodynamic viewpoint. Fig.S3 illustrates two representative temperature-composition (T-X) diagrams. Fig.S3A shows T-X diagram of naphthalene and benzene. As can be seen from this T-X diagram, solid naphthalene and solid benzene are not soluble for each other, so that no **solid solutions** are formed. On cooling the **liquid solution** from Point X', recrystallization of naphthalene begins to take place at Point P. On further cooling, the **liquid solution** completely disappears at Point Q and a mixture of solid naphthalene and solid benzene begins to form. Fig.S3B shows a part of T-X diagram of aluminium and copper. Solid aluminium and solid copper are partially soluble for each other, so that the **solid solutions** α and θ are formed, as can be seen from this diagram. On cooling the **liquid solution** from Point X', recrystallization of **solid solution** α begins to take place at Point P and **liquid solution** completely disappears at Point Q. On further cooling, phase separation begins at Point R to form a mixture of **solid solutions** α and θ. We look at a dotted line in Fig.13. On cooling **solid solution** along this dotted line, phase separation begins at Point R to form a mixture of **solid solution** and solid carbon (CNT). With decreasing temperature, the more carbons supersaturate in the solid solution, the more solid carbon (CNT) separate from the **solid solution**.

As can be seen from Fig. 13, solubility of carbon in the metal-carbon solid solution apparently depends on metal and temperature: the best solubility of Ni is 2.7% at *ca.*1460°C; Co, 4.1% at *ca.* 1320°C; Fe, 0.1% at 740°C (and 9.06% at 1153°C

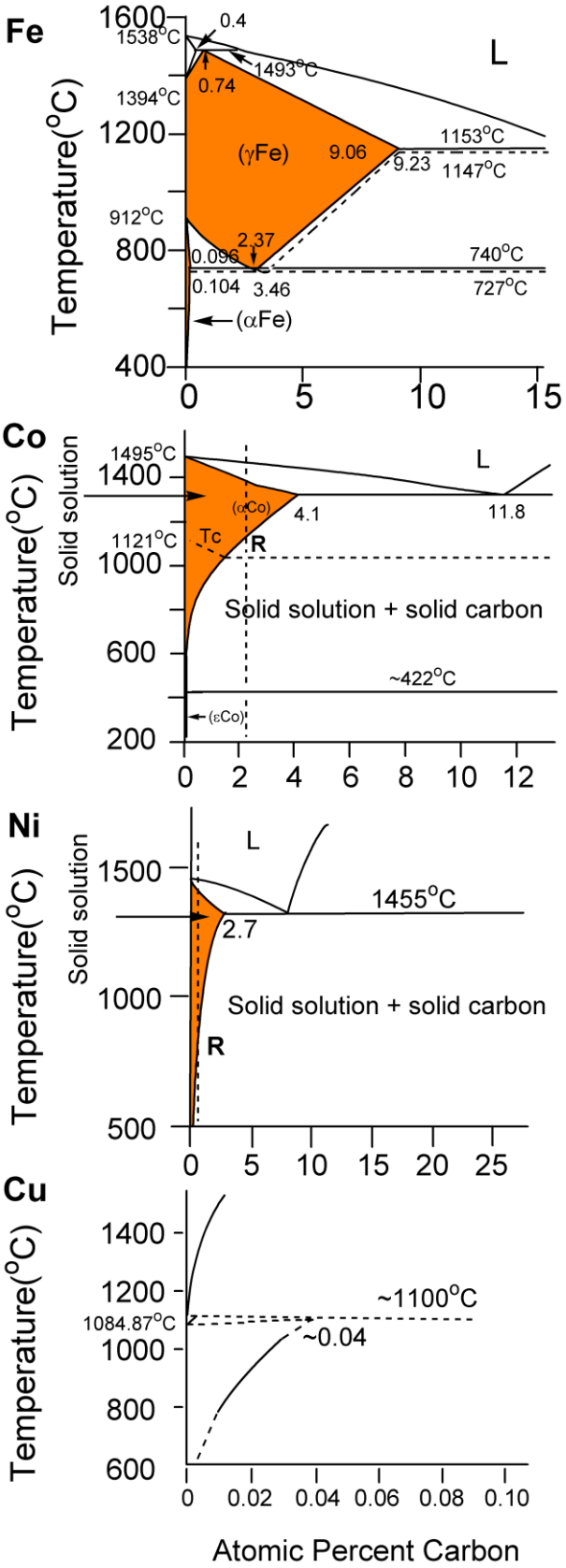

Fig. 13. Temperature-composition (T-X) diagrams of metal–carbon binary system for Fe, Co, Ni and Cu. Coloured area represents solid solution.

This journal is © The Royal Society of Chemistry [year]

for γFe). Therefore, amount of saturated carbon in a nanoparticle of the metal-carbon solid solution depends on the nanoparticle volume. The volume of nickel nanoparticle rapidly increases in proportion to the third power of the diameter. The bigger the nickel nanoparticle diameter becomes, the more amount of carbon resolves in a nickel nanoparticle. Accordingly, the more carbon products can be formed from the bigger nickel nanoparticles. Thus, the bigger the catalytic nickel nanoparticle becomes, the thicker the carbon nanotube is resulted. As mentioned above, we found a good linear correlation between the diameter ($\mathbf{D_{Ni}}$) of the catalytic nickel nanoparticles and the outer diameter ($\mathbf{D_{CNT}}$) of the resulted carbon nanotubes. Fig.14 illustrates the relationship between outer diameter of CNTs and the diameter of catalytic nickel nanoparticles. From the thermodynamic viewpoint discussed above, we believe that the present relationship may be widely applicable to all the CNTs prepared by other techniques. As a matter of fact, the CNTs prepared by CVD methods also showed the same liner relationship in a region of diameters of the catalytic metal nanoparticles ($\mathbf{D_M}$ = 1.0~12.6 nm),[14] as already mentioned above.

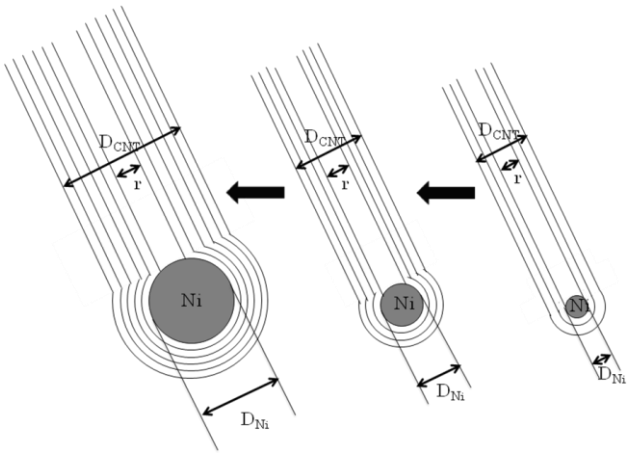

Fig.14 Relationship between outer diameter of CNTs and the diameter of catalytic nickel nanoparticles. The bigger the nickel nanoparticle becomes, the thicker the resulted carbon nanotube becomes.

4. CONCLUSION

We have rapidly synthesized MWCNTs by calcination of granulated polystyrene with nickel nanoparticles having different diameter ($\mathbf{D_{Ni}}$ = 10, 20, 50 or 90 nm), under nitrogen gas using a domestic microwave oven. We revealed that outer diameter of the obtained MWCNTs ($\mathbf{D_{CNT}}$) increases by about 1 nm when diameter of the catalytic metal nanoparticles ($\mathbf{D_{Ni}}$) increases by 1 nm. To our best knowledge, such a good linearity between $\mathbf{D_M}$ and $\mathbf{D_{CNT}}$ has been established at the first time in the very wide range of diameter of catalytic metal nanoparticles from 1nm to 90nm.

Acknowledgements

This work was financially supported by Grant-in-Aid for Challenging Exploratory Research (Grant Number 25620142) from Japan Society for the Promotion of Science.

Notes and references

[a] *Smart Material Science and Technology, Interdisciplinary Graduate School of Science and Technology, Shinshu University, 3-15-1 Tokida, Ueda 386-8567, Japan. TEL&Fax: +81-(0)268-21-5492; E-mail: ko52517@shinshu-u.ac.jp*

[b] *Applied Chemistry Course, Division of Chemistry and Materials, Faculty of Textile Science and Technology, Shinshu University, 3-15-1 Tokida, Ueda 386-8567, Japan. E-mail: hattoriy@shinshu-u.ac.jp*

[c] *Nippon Steel & Sumikin Chemical Co., Ltd., 14-1 Sotokanda, Chiyoda-ku, Tokyo 101-0021, Japan. E-mail: konotk@nscc.nssmc.com*

† Electronic Supplementary Information (ESI) available: [details of any supplementary information available should be included here]. See DOI: 10.1039/b000000x/

‡ Parts 1, 2 and 3: Refs. 10, 11 and 12 in this paper, respectively.

1 "*Chemical Frontier 2, Carbon Nanotubes - Challenge to Nano Devices (= Kagaku Furontya 2, Kabon Nanotubu – Nano Debaisu heno Chosen (in Japanese))*" ed., Kazuyoshi Tanaka, 2001, Kagaku Dojin (Kyoto).

2 "*Basis and Applications of Carbon Nanotubes (= Kabon Nanotubu no Kiso to Ohyo (in Japanese))*", ed., Ri-ichiro Saito and Hisanori Shinohara, 2004, Baifukan (Tokyo).

3 S. Iijima, *Nature*, 1991, **354**, 56.

4 S. A. Majetich, J. O. Artman, M. E. McHenry, N. T. Nuhfer and S. W. Staley, *Phys. Rev. B.*, 1993, **48**, 16845.

5 T. Hayashi, S. Hirono and M. Tomita, *Nature*, 1996, **381**, 772.

6 P. J. F. Harris and S. C. Tsang, *Chem. Phys. Lett*., 1998, **293**, 53.

7 A. Thess, P. Nikolaev, H. J. Dai, P. Petit, J. Robert, C. H. Xu, Y. H. Lee, S. G. Kim, A. G. Rinzler, D. T. Cobert, G. E. Scuseria, D. T. Tomanek, J. E. Fisher and R. E. Smalley, *Science*, 1996, **273**, 483.

8 M. Endo, K. Takeuchi, S. Igarashi, K. Kobori, M. Shiraishi and H. W. Kroto, *J. Phys. Chem. Solids*, 1993, **54**, 1841.

9 B. H. Liu, J. Ding, Z. Y. Zhong, Z. L. Dong, T. White and J. Y. Lin, *Chem. Phys. Let*t., 2002, **358**, 96.

10 Y. Takagaki, H.-D. Nguyen-Tran and K. Ohta, *Bull. Chem. Soc. Jpn.*, 2010, **83**, 1100.

11 T. Ohta, T. Ito, M. Shimizu, L. Tauchi, H.-D. Nguyen-Tran, J.-C. Park, B.-S. Kim, I.-S. Kim and K. Ohta, *Polym. Adv. Technol.*, 2010, **21**, 1: (www.interscience.wiley.com) DOI: 10.1002/pat.1723.

12 Y. Takagi, L. Tauchi, H.-D. Nguyen-Tran, T. Ohta, M. Shimizu and K. Ohta. *J. Mater. Chem*., 2011, **21**, 14569.

13 C. Laurent, E. Flahaut, A. Peigney and A. Rousset, *New. J. Chem.*, 1998, 1229.

14 E. Lamouroux, P. Serp and P. Kalck, *Cat. Rev.*, 2007, **49**, 341.

15 J.-P. Tessonnier and D. S. Su, *ChemSusChem.*, 2011, **4**, 824.

16 Y. Tsukahara, Y. Wada, T. Yamauchi, A. Baba, M. Yasuda, T. Sakamoto, T. Kono and R. Kawabata, *Jpn. Kokai Tokkyo Koho*, JP2010-64983(A)-2010-03-25 (Priority number: JP2008-232863; Submission Date: 2008-09-11); T. Yamauchi, Y. Tsukahara, T. Sakamoto, T. Kano, M. Yasuda, A. Baba and Y. Wada, *Bull. Chem. Soc. Jpn.*, 2009, **82**, 1044.

17 The small furnace for domestic microwave oven is called as Art Box™ in Japan and Microkiln™ in USA.

18 *"Binary Alloy Phase Diagrams, 2nd Edition"*, ed. T. B. Massalski, H. Okamoto, P. R. Subramanian, L. Kacprzak, ASM International, 1990.